J MATER RES TECHNOL. 2017;xxx(xx):xxx–xxx

Available online at www.sciencedirect.com

jmr&t Journal of Materials Research and Technology

www.jmrt.com.br

Original Article

Corrosion inhibition effect of non-toxic α-amino acid compound on high carbon steel in low molar concentration of hydrochloric acid

Roland Tolulope Loto

Department of Mechanical Engineering, Covenant University, Ota, Ogun State, Nigeria

ARTICLE INFO

Article history:
Received 1 August 2017
Accepted 6 September 2017
Available online xxx

Keywords:
Corrosion
Steel
HCl
Adsorption
Inhibitor

ABSTRACT

Electrochemical studies of the corrosion inhibition effect of biodegradable 2-amino-4-methylpentanoic acid (LCN) on high carbon steel in 1M HCl acid was evaluated with potentiodynamic polarization technique, weight loss analysis and optical microscopy. Results show the compound to be highly effective with optimal inhibition efficiencies of 87.46% and 85.88% from the electrochemical test with dominant cathodic inhibition behaviour between 0% and 1.88% inhibitor concentration and anodic inhibition behaviour at 2.81% and 5.63% inhibitor concentration due to changes in the effect of lateral repulsion between inhibitor molecules. Thermodynamic calculations showed chemisorption molecular interaction and adsorption onto HCS surface according to Langmuir, Freundlich and Frumkin isotherm models with correlation coefficients of 0.9991, 0.8727 and 0.9782. Statistical analysis showed inhibitor concentration is only relevant variable responsible for inhibition efficiency. Calculated results from predicted corrosion rate values varied at an average value of 53% from experimental results. Optical microscopy images of LCN inhibited and uninhibited HCS samples significantly contrast each.

1. Introduction

Ferrous alloys are extensively applied in industry such as petrochemical, chemical processing, pharmaceuticals, marine, automobile, mining and extraction, energy and construction industries, etc., as materials of construction for equipment, machines, devices and plants structures. Most industrial environments are highly corrosive to these alloys during application, e.g., hydrochloric acid is used in the petroleum industry for oil well acidizing and in the mining and extraction for pickling and removal of metals from their ores. In most cases, corrosion problems are associated with operating problems and equipment maintenance, leading sometimes to recurrent, partial and even total process shutdown resulting in severe financial and economic losses. They often appear as leaks, rust, pitted holes and deteriorations in tanks, casings, tubing, pipelines, and other equipment. The use of corrosion inhibiting chemicals known as inhibitors has been proven to be one of the most practical techniques of corrosion protection of metals in anion

E-mail: tolu.loto@gmail.com

http://dx.doi.org/10.1016/j.jmrt.2017.09.005

Please cite this article in press as: Loto RT. Corrosion inhibition effect of non-toxic α-amino acid compound on high carbon steel in low molar concentration of hydrochloric acid. J Mater Res Technol. 2017. http://dx.doi.org/10.1016/j.jmrt.2017.09.005

containing industrial environments such as acid cleaning, oil well acidification, acid pickling and descaling processes [1–4]. Previous research on the use of organic compounds as metallic corrosion inhibitors in acid solutions attests to their generally high performance characteristics; however, their use is limited by their varying levels of toxicity, thus the need for environmentally sustainable substitutes [5–13]. Amino acids belong to the class of non-toxic organic compounds which are highly soluble in aqueous media, rapidly biodegradable and easily produced at high purity with low cost. Their derivatives have been used in previous research experimentations to inhibit the corrosion of metals and alloys [14–25]. They contain heteroatoms such as nitrogen, sulphur and oxygen, in addition to multiple bonds in their structure which facilitate adsorption onto metallic surfaces. Their corrosion inhibition performance is subject to their molecular size, molecular mass, internal structure, heteroatoms and adsorption strength. 2-Amino-4-methylpentanoic acid, is an essential branched-chain α-amino acid containing α-amino group, α-carboxylic acid group, an isobutyl side chain and an aliphatic side-chain that is non-linear. It is used in the biosynthesis of proteins in animals and is important for haemoglobin formation. In continuation of inhibitor development and the drive for improved efficiency, this research aims to study and evaluate the electrochemical performance of 2-amino-4-methylpentanoic acid on high carbon steel in dilute hydrochloric acid.

2. Experimental methods

High carbon steel (HCS) obtained commercially has a nominal (wt%) composition as shown in Table 1. The steel specimen were abraded with silicon carbide papers (80, 320, 600, 800 and 1000 grit) after machining, before cleansing with deionized water and acetone, and kept in a desiccator for electrochemical test and corrosion potential measurement according to ASTM G1-03 [26]. The polarization plots were obtained at a scan rate of 0.0015 V/s between potentials of −0.5 V and +1 V according to ASTM G102-89 [27]. A platinum rod was used as the counter electrode and a silver chloride electrode (Ag/AgCl) as the reference electrode. Corrosion current density (J_{corr}) and corrosion potential (E_{corr}) values were obtained using the Tafel extrapolation method. The corrosion rate (C_R) and the inhibition efficiency (η, %) were calculated from the mathematical relationship;

$$C_R = \frac{0.00327 \times J_{corr} \times E_{qv}}{D} \quad (1)$$

J_{corr} is the current density in A/cm^2, D is the density in g/cm^3; E_{qv} is the sample equivalent weight in grams. 0.00327 is a constant for corrosion rate calculation in mm/y [28]. L-2-Amino-4-methylpentanoic acid (LCN) obtained from Sigma Aldrich, USA is a white powdery solid whose molecular structure is shown in Fig. 1. It has a molar mass of 131.17 g/mol. 200 mL of 1 M HCl/0.91%, 1.88%, 2.81%, 3.75%, 4.69% and 5.63% LCN prepared from analar grade of HCl acid (37%) with deionized water. Optical images of steel samples before and after corrosion were analyzed with Omax trinocular metallurgical through the aid of ToupCam analytical software.

Table 1 – Percentage nominal composition of HCS.

Element symbol	Mn	P	S	C	Fe
% Composition (1018CSS)	0.7	0.04	0.05	0.70	98.51

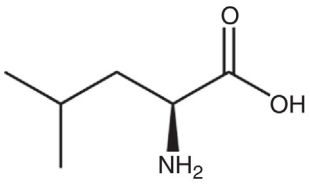

Fig. 1 – Molecular structure of LCN compound.

Measured HCS coupons separately immersed in 200 mL of the dilute acid test solution for 288 h at 30 °C were weighed at 24 h interval according to ASTM G31-72 [29]. Corrosion rate (C_R) is determined as follows as [30];

$$C_R = \left[\frac{87.6\omega}{DAt}\right] \quad (2)$$

ω is the weight loss in mg, D is the density in g/cm^3, A is the total surface area of the coupon in cm^2 and 87.6 is a constant for corrosion rate determination in mm/y. t is the time in h. Inhibition efficiency (η) was determined from the equation below;

$$\eta = \left[\frac{\omega_1 - \omega_2}{\omega_1}\right] \times 100 \quad (3)$$

ω_1 and ω_2 are the mass loss at specific LCN concentrations. Surface coverage was determined from the relationship [31,32]:

$$\theta = \left[1 - \frac{\omega_2}{\omega_1}\right] \quad (4)$$

where θ is the degree of LCN compound, adsorbed per gram of HCS samples. ω_1 and ω_2 are the weight loss of each HCS sample at specific concentrations of LCN in the acid solution.

3. Results and discussion

3.1. Potentiodynamic polarization studies

The potentiodynamic polarization scans for the active-passive electrochemical corrosion behaviour of HCS in HCl at 0%–5.63% LCN are shown in Fig. 2. Numerical results of the polarization scans are presented in Table 2. The corrosion potentials of the polarization plots shifts from −0.256 V at 0% LCN to cathodic values of −0.267 V and −0.269 V at low LCN concentrations of 0.91% and 1.88% LCN due to the dominant cathodic inhibiting action of protonated LCN molecules on HCS surface whereby the hydrogen evolution and oxygen reduction reactions are effectively suppressed. This shift in corrosion potential is also due to an active site blocking effect that occurs when an inhibitor is added to a corrosive solution [33]. It is likely the available LCN molecules at the earlier mentioned concentrations precipitated on specific sites on the

Please cite this article in press as: Loto RT. Corrosion inhibition effect of non-toxic α-amino acid compound on high carbon steel in low molar concentration of hydrochloric acid. J Mater Res Technol. 2017. http://dx.doi.org/10.1016/j.jmrt.2017.09.005

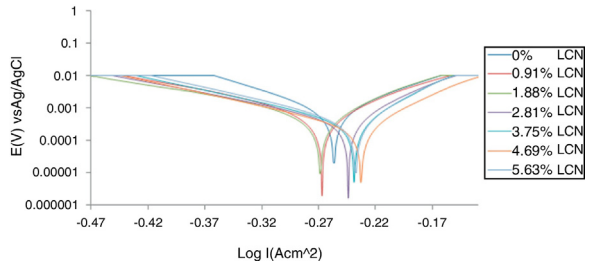

Fig. 2 – Potentiodynamic polarization plots for HCS in (0–5.63% LCN) 1 M HCl.

steel's surface during the inhibition process thereby increasing the surface impedance of the steel. Further increase in LCN concentration (2.81%–5.63% LCN) proportionally shifts the corrosion potential values to anodic potentials probably as a result of total surface coverage by the excess LCN molecules causing inhibition of the surface oxidation of HCS by steric hindrance to the cathodic and mainly the anodic reactions.

Variation in corrosion rate for HCS at 0% LCN and (0.91%–5.63% LCN) is fundamentally due to the adsorption of LCN compound on HCS surface, thus improving the passivity of the HCS in HCl. The corrosion rates and corrosion current density decreased significantly with increase in LCN concentration. Changes in LCN concentration had no significant effect on the cathodic Tafel slopes between 0.91% and 1.88% LCN. The anodic Tafel slopes are observed to be greater than the respective cathodic Tafel slopes. This is as a result of the anodic exchange-current density values being lesser than those of the cathodic values. The anodic Tafel value at 0% LCN is the product of oxide formation on HCS surface oxides due to the slow electron transfer step [34,35]. Changes in anodic Tafel slope values after 0% LCN and is due to changes in the electrode substrate, rate controlling step and influence of potential controlled conditions resulting from the electrochemical action of LCN. This is further proven from the inhibition efficiency, whose values marginally increased in proportion to concentration. The increase of inhibitor efficiency with increasing of the concentration can be interpreted on the basis of the adsorption amount and the coverage of surfactant molecules, increases with increasing concentrations as earlier mentioned [36]. The maximum change in corrosion potential of HCS for both the anodic and cathodic direction is less than 85 mV; hence LCN is a mixed type inhibitor in HCl solution.

3.2. *Inhibition mechanism of LCN*

Amino acids are organic compounds containing amine ($–NH_2$) and carboxyl (–COOH) functional groups, along with a side chain (R group) due to their amphiprotic nature specific to amino acids. LCN being a weak acid releases a proton at low concentrations in the acid solution. During electrochemical reaction the carboxylic acid functional groups ($–CO_2H$) deprotonates to become negative carboxylates ($–CO_2^-$) while the α-amine functional group (NH_2^-) protonates to become positive α-ammonium groups ($+NH_3^-$). The positively charged α-ammonium group predominates at low concentrations while the negatively charged carboxylate ion predominates at higher concentrations. Lone pair of electrons is available on the nitrogen and oxygen atoms; hence coordination of amino acids with metal atoms occurs through these atoms. The flow of electrons from the electron rich centres of LCN to electron deficient centres of HCS metal inhibits the electrochemical processes responsible for corrosion. The observed increase in inhibition efficiency of LCN with increase in concentration, suggests LCN adsorbs on HCS.

3.3. *Weight-loss measurement and optical microscopy analysis*

Experimental results for weight-loss (ω) and corrosion rate (C_R) of HCS, and LCN inhibition efficiency (η) in 1 M HCl solution at 288 h exposure time are presented in Table 3. Fig. 3(a) and (b) shows the graphical plot of HCS corrosion rate and LCN inhibition efficiency versus exposure time during the exposure period. Optical microscopic images of HCS before corrosion, and after corrosion with and without LCN inhibiting compound are shown from Fig. 4(a) to 5(b) at mag. 40×. The corrosion rate of HCS at 0% LCN [Fig. 3(a)] decreased for the first 72 h of exposure to 0.0081 mm/y before increasing progressively to 0.0111 mm/y at 288 h during which severe surface oxidation of HCS occurred as depicted by the surface morphology in Fig. 4(b). Numerous micro and macro-pits coupled with a porous texture consisting of hydrated iron (III) oxides and iron (III) oxide-hydroxide. This observation is due to the electrochemical action of Cl^- ions, resulting from the disassociation of HCl in H_2O according to the equation below;

$$HCl_{(aq)} + H_2O_{(l)} \rightarrow H_3O^+_{(aq)} + Cl^-_{(aq)} \quad (5)$$

The Cl^- ions in solution reacts with HCS according to the following equation causing the rapid oxidation of HCS

$$Fe_{(s)} + 2HCl_{(aq)} \rightarrow FeCl_{2(aq)} + H_{2(g)} \quad (6)$$

Continuous deterioration and oxide formation of HCS lead to the formation of pores and channels within the oxide layer which further accelerates the corrosion of the steel. At 0.91% LCN to 5.63% LCN, the corrosion rate of HCS decreased significantly from the onset of the exposure hours (24 h) till 288 h due to the action of LCN molecules in retarding the redox electrochemical reaction of Cl^- ions. The optical micrograph in Fig. 5(a) and (b) shows a mildly deteriorated morphology at 0.91% LCN and 5.63% LCN in comparison to Fig. 4(b) due to the electrochemical interaction between the Cl^- ions and inhibitor cations. The inhibition efficiency of LCN seems to be more time dependent than its concentration value as its inhibition efficiency tends to increase with time [Fig. 3(b)] at all concentrations studied to peak at values between 72.35% and 85.88% at 288 h. Due to the presence of N and O heteroatom in its molecular structure, the α-amino groups (NH_2^-) protonates to become positive α-ammonium groups ($+NH_3^-$) in the acid solution and inhibits further corrosion of HCS through adsorption via the negatively charged chloride ions, resulting in the pi electrons and unshared electrons pairs forming a strong bond with vacant d-orbital of HCS surface. In the presence of LCN compound, transition from active deterioration of

Please cite this article in press as: Loto RT. Corrosion inhibition effect of non-toxic α-amino acid compound on high carbon steel in low molar concentration of hydrochloric acid. J Mater Res Technol. 2017. http://dx.doi.org/10.1016/j.jmrt.2017.09.005

Table 2 – Potentiodynamic polarization result for HCS in 1 M HCl (0%–5.63% LCN) acid solution.

Sample	LCN conc. (%)	LCN conc. (M)	HCS corrosion rate (mm/y)	LCN inhibition efficiency (%)	Corrosion current (A)	Corrosion current density (A/cm^2)	Corrosion potential (V)	Polarization resistance, R_p (Ω)	Cathodic Tafel slope, B_c (V/dec)	Anodic Tafel slope, B_a (V/dec)
A	0	0	22.13	0	2.94E−03	1.91E−03	−0.256	19.65	−7.533	10.770
B	0.91	6.96E−02	6.22	71.90	8.26E−04	5.36E−04	−0.267	40.61	−7.375	14.950
C	1.88	1.43E−01	5.36	75.76	7.12E−04	4.62E−04	−0.269	51.25	−7.541	14.080
D	2.81	2.14E−01	4.37	80.23	5.81E−04	3.77E−04	−0.244	70.65	−8.156	13.380
E	3.75	2.86E−01	4.08	81.58	5.41E−04	3.51E−04	−0.239	91.26	−8.183	13.230
F	4.69	3.57E−01	2.92	86.80	3.88E−04	2.52E−04	−0.237	123.67	−8.317	13.850
G	5.63	4.29E−01	2.78	87.46	3.68E−04	2.39E−04	−0.233	146.91	−8.542	13.420

Please cite this article in press as: Loto RT. Corrosion inhibition effect of non-toxic α-amino acid compound on high carbon steel in low molar concentration of hydrochloric acid. J Mater Res Technol. 2017. http://dx.doi.org/10.1016/j.jmrt.2017.09.005

Table 3 – Results from weight loss analysis at 240 h for HCS in 1 M HCl solution (0%–5.63% LCN).

Samples	LCN concentration (%)	LCN concentration (molarity)	Weight loss (g)	Corrosion rate (mm/y)	LCN inhibition efficiency (%)
A	0	0	1.703	0.0111	0
B	0.91	6.96E−02	0.471	0.0031	72.35
C	1.88	1.43E−01	0.424	0.0028	75.10
D	2.81	2.14E−01	0.293	0.0019	82.82
E	3.75	2.86E−01	0.288	0.0019	83.09
F	4.69	3.57E−01	0.255	0.0017	85.02
G	5.63	4.29E−01	0.240	0.0016	85.88

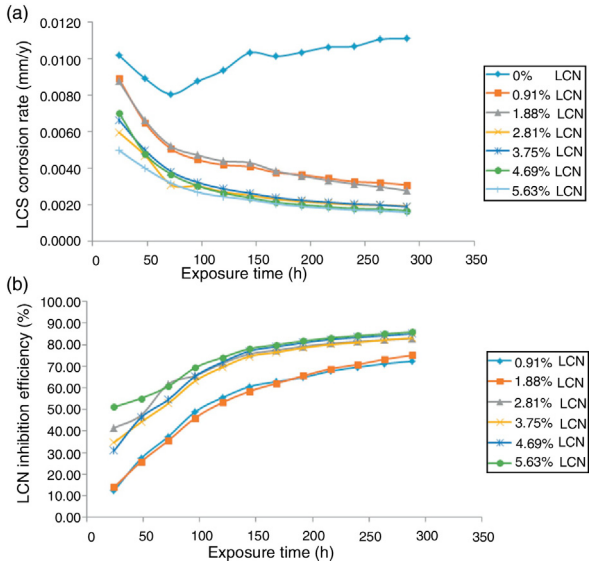

Fig. 3 – Plot of (a) HCS corrosion rate versus exposure time in 1 M HCl. (b) LCS inhibition efficiency versus exposure time in 1 M HCl.

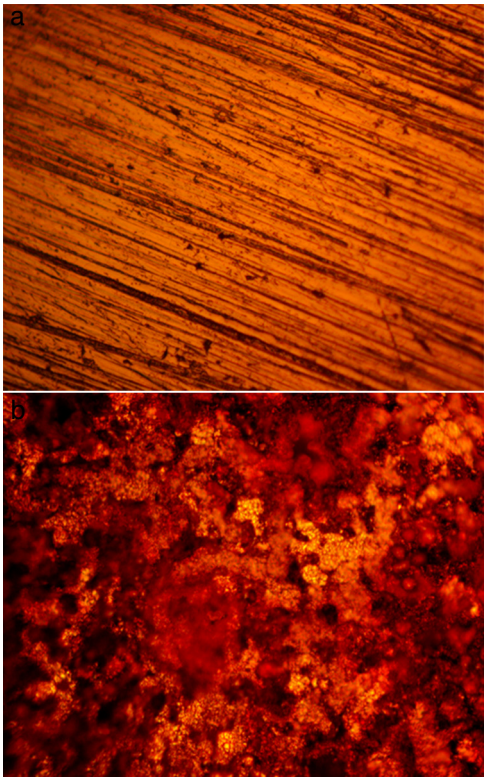

Fig. 4 – Optical microscopic image of HCS at mag. 40× (a) before corrosion, (b) after corrosion in 0% LCN/1 M HCl.

HCS surface to the passive state was gradual due to the time dependent action of LCN adsorption on HCS. LCN inhibition attained 70% efficiency between 96 and 120 h for 2.81%–5.63% LCN concentration. LCN inhibitor at 0.91% and 1.88% concentration attained 70% efficiency at about 240 h.

3.4. *Adsorption Isotherm*

The inhibition efficiency of chemical compounds is due to the strength of its adsorption on metallic surfaces in corrosive media. Adsorption depends upon the orientation of the inhibitor molecule, and its ionization and polarization [37]. The interaction of inhibitor molecules on metallic surfaces resulting from the aggregation and formation of molecular film on metallic surfaces can be further understood through adsorption isotherms. The isotherms show the phenomenon governing the retention of substances from aqueous solution to solid interphase at a constant temperature and pH [38,39]. Langmuir, Freundlich and Frumkin gave the best fitting for LCN adsorption on HCS in HCl as shown from Figs. 6–8.

Plots of C_{LCN}/θ vs C_{LCN} fits with the Langmuir isotherm (Fig. 6), with a correlation coefficient of 0.9991 according to the Langmuir equation below.

$$\theta = \left[\frac{K_{LCN}C_{LCN}}{1 + K_{ads}C_{LCN}}\right] \quad (7)$$

θ is the amount of LCN adsorbed per unit gram on HCS surface at equilibrium. C_{LCN} is LCN concentration and K_{ads} is the equilibrium constant of adsorption. The high values of K_{ads} indicate strong adsorption on HCS surface in HCl solution due to the presence of donor atoms of nitrogen in LCN functional groups [40]. Langmuir isotherm assumes that there are fixed number of vacant or adsorption sites available on the metal surface, these sites are of equal dimension and shape on the metal surface, each site can hold a definite amount of molecule resulting in a constant amount of heat energy is released and no lateral interaction between the adsorbed molecules exists [41].

Please cite this article in press as: Loto RT. Corrosion inhibition effect of non-toxic α-amino acid compound on high carbon steel in low molar concentration of hydrochloric acid. J Mater Res Technol. 2017. http://dx.doi.org/10.1016/j.jmrt.2017.09.005

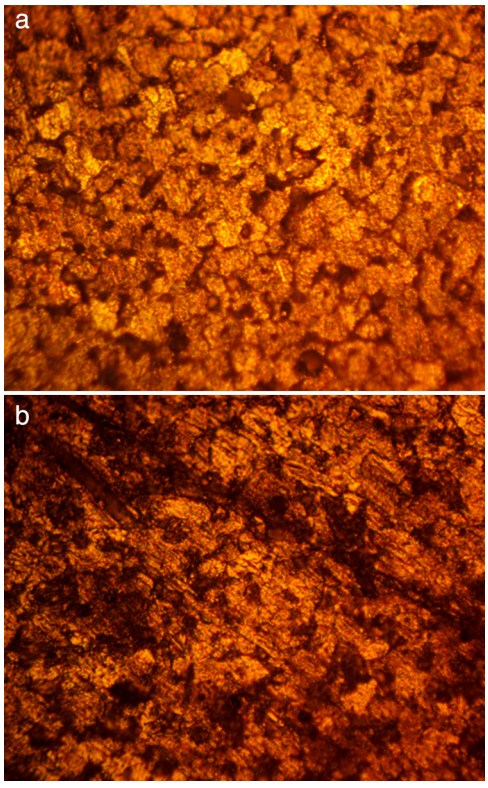

Fig. 5 – Optical microscopic image of HCS at mag. 40× (a) after corrosion in 0.91% LCN/1 M HCl, (b) after corrosion in 5.63% LCN/1 M HCl.

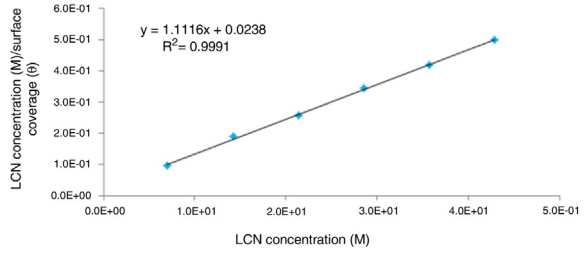

Fig. 6 – Langmuir plot of C_{LCN}/θ versus LCN concentration in 1 M HCl.

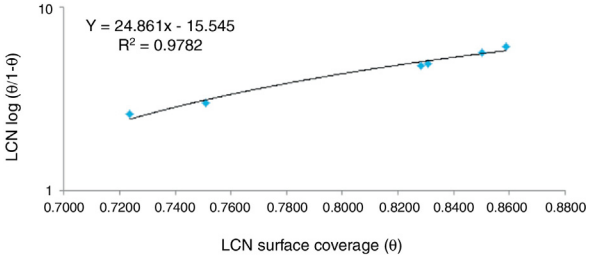

Fig. 7 – Frumkin isotherm plot of log[θ/(1 – θ)c] versus θ 1 M HCl.

The Frumkin adsorption isotherm assumes metallic surfaces to be heterogeneous and the lateral interaction effect among the adsorbed molecules is apparent according to the equation [42]:

$$\frac{\theta}{1-\theta} = Kc\,e^{2\alpha\theta}, \text{rearranging the equation becomes} \quad (8)$$

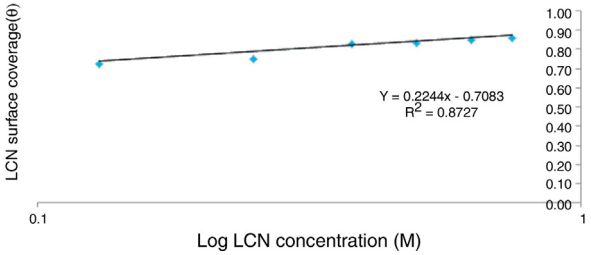

Fig. 8 – Freundlich isotherm plot of log LCN concentration vs log surface coverage.

$$\log\left[\frac{\theta}{(1-\theta)c}\right] = 2.303\,\log K + 2\alpha\theta \quad (9)$$

α is the interaction parameter which describes the molecular interaction in adsorbed layer, and calculated from the slope of the Frumkin isotherm plot. Taking into account, the attraction ($\alpha > 0$), repulsion ($\alpha < 0$) and no interaction ($\alpha = 0$) between the adsorbed species, the isotherm becomes equivalent to the Langmuir isotherm. For +ve α, adsorption energy increases with θ, whereas for negative α adsorption energy decreases with θ. K is the adsorption–desorption constant. Plots of log[θ/(1 – θ)c] versus θ in Fig. 7 showed a correlation coefficient of 0.9782 in HCl.

Freundlich isotherm shows the relationship between adsorbed molecules, their interaction and influence on the adsorption process through molecular repulsion or attraction according to the following equation.

$$\theta = KC^n \quad (10)$$

$$\log\theta = n\,\log C + \log K_{ads} \quad (11)$$

where n is a constant depending on the characteristics of the adsorbed molecule, K_{ads} is the adsorption–desorption equilibrium constant denoting the strength of interaction in the adsorbed layer. The amount adsorbed on HCS surface represents the sum total of adsorption on the reactive sites [43,44]. The correlation coefficient for Freundlich isotherm plot (Fig. 8) is 0.8727.

3.5. *Thermodynamics of the corrosion inhibition mechanism*

The strength and type of adsorption of the corrosion inhibition mechanism of LCN on HCS was determined from the thermodynamics of LCN molecular interaction with the steel surface through the equilibrium constant of adsorption of the Langmuir isotherm due to its correlation coefficient approaching unity. Calculated results of Gibbs free energy of adsorption in HCl solution is shown in Table 4, from Eq. (12) [45].

$$\Delta G_{ads} = -2.303\,RT\,\log[55.5K_{ads}] \quad (12)$$

where 55.5 is the molar concentration of water in the acid solution, R is the universal gas constant, T is the absolute temperature and K_{ads} is the equilibrium constant of adsorption. Negative values of ΔG^{o}_{ads} signify spontaneous and stable

Please cite this article in press as: Loto RT. Corrosion inhibition effect of non-toxic α-amino acid compound on high carbon steel in low molar concentration of hydrochloric acid. J Mater Res Technol. 2017. http://dx.doi.org/10.1016/j.jmrt.2017.09.005

Table 4 – Results for Gibbs free energy (ΔG^{o}_{ads}), surface coverage (θ) and equilibrium constant of adsorption (K_{ads}) for LCN adsorption on HCS in 1 M HCl solution.

Samples	LCN concentration (M)	Surface coverage (θ)	Equilibrium constant of adsorption (K)	Gibbs free energy, ΔG (kJ mol^{-1})
A	0	0	0	0
B	6.96E−02	0.724	37 620.5	−36.06
C	1.43E−01	0.751	21 094.4	−34.63
D	2.14E−01	0.828	22 476.2	−34.78
E	2.86E−01	0.831	17 182.2	−34.12
F	3.57E−01	0.850	15 878.6	−33.92
G	4.29E−01	0.859	14 183.4	−33.64

adsorption reactions. In HCl solution, the lowest ΔG^{o}_{ads} value is −33.64 kJ mol^{-1}, at the highest LCN concentration and the highest ΔG^{o}_{ads} value of −36.06 kJ mol^{-1} occurred at the lowest LCN concentration on HCS surface. These ΔG^{o}_{ads} values in HCl solution depict chemisorption adsorption reaction mechanisms, i.e., chemical interaction of LCN molecules through charge sharing and covalent bonding on the steel's surface. The chemisorption of the LCN cationic molecules could also occur due to the interaction between the d orbital of the oxidized HCS surface which involved displacement of H_2O molecules from the metal surface, and the lone sp^2 electron pairs present on the N, atoms of LCN [46,47]. The result also shows that lateral interaction according to Frumkin adsorption isotherm among the inhibitor species tends to be repulsive with increase in LCN concentration hence the decrease in ΔG^{o}_{ads} value.

3.6. *Analysis of variance*

Statistical analysis at a confidence level of 95% (significance level of $\alpha = 0.05$) was used to calculate the statistical significance of LCN concentration and time of exposure on LCN inhibition efficiency results from weight loss throughout the exposure period of 288 h according to Eqs. (13)–(15).

The sum of squares among columns (LCN concentration)

$$SS_c = \frac{\sum T_c^2}{nr} - \frac{T^2}{N} \quad (13)$$

Sum of squares among rows (time of exposure)

$$SS_r = \frac{\sum T_r^2}{nc} - \frac{T^2}{N} \quad (14)$$

Total sum of squares

$$SS_{Total} = \sum x^2 - \frac{T^2}{N} \quad (15)$$

Table 6 – Comparison of predicted and experimental corrosion rate results.

LCN concentration (%)	Experimental corrosion rate (mm/y)	Predicted corrosion rate (mm/y)
0	0.0111	0.0059
0.91	0.0031	0.0016
1.88	0.0028	0.0015
2.81	0.0019	0.0010
3.75	0.0019	0.0010
4.69	0.0017	0.0009
5.63	0.0016	0.0008

Results from statistical analysis in Table 5 showed that LCN inhibitor concentration is the only statistically relevant variable responsible for LCN inhibition efficiency results with significance factor value (F-value) of 37.12 in HCl solution [48]. These values are much greater than the control significance factor (significance F) value of 2.42, corresponding to a percentage significance of 119.2. The effect of LCN inhibitor concentration on inhibition efficiency values is deemed unlikely to have occurred by chance, but significantly influenced the performance of LCN inhibitor as against the time of exposure. The results show that changes in LCN concentration has strong influence the electrochemical corrosion behaviour and inhibitor protection of LCN on HCS in contrast to exposure time whose results show it is statistically irrelevant. LCN is a concentration dependent inhibitor.

3.7. *Theoretical model for corrosion rate*

Corrosion rates values have been known not to be fixed values due to the unpredictable nature of corrosion [49]. Most often the corrosion process is often controlled by stochastic phenomena; as a result, mathematical models with appropriate mathematical equations can be used to accurately predict the corrosion rate of metals before the corrosion occurs. The theoretical corrosion rate model used was developed by dimensional analysis using the Buckingham–Pie technique to obtain the expression for the theoretical corrosion rate model as [50–53];

$$C_{Rm} = D_f\left(\frac{VT\mu}{AD}\right) \quad (16)$$

where D is the density of the fluid, V is the velocity of the fluid, μ is the viscosity of the fluid, T is the exposure time and A is the area of the specimen. D_f is the dimensionless corrosion rate

Table 5 – Analysis of variance for LCN inhibition efficiency on HCS in 1 M HCl at 95% confidence level.

Source of variation	Sum of squares	Degree of freedom	Mean square	Mean square ratio (F)	Significance F (min. MSR at 95% confidence)	F (%)
LCN concentration	315 583.48	5	63 116.70	37.12	2.53	119.2
Exposure time	−144 278.13	11	−13 116.19	−7.71	2.42	−54.5
Residual	93 530.79	55	1700.56			
Total	264 836.15	71				

Please cite this article in press as: Loto RT. Corrosion inhibition effect of non-toxic α-amino acid compound on high carbon steel in low molar concentration of hydrochloric acid. J Mater Res Technol. 2017. http://dx.doi.org/10.1016/j.jmrt.2017.09.005

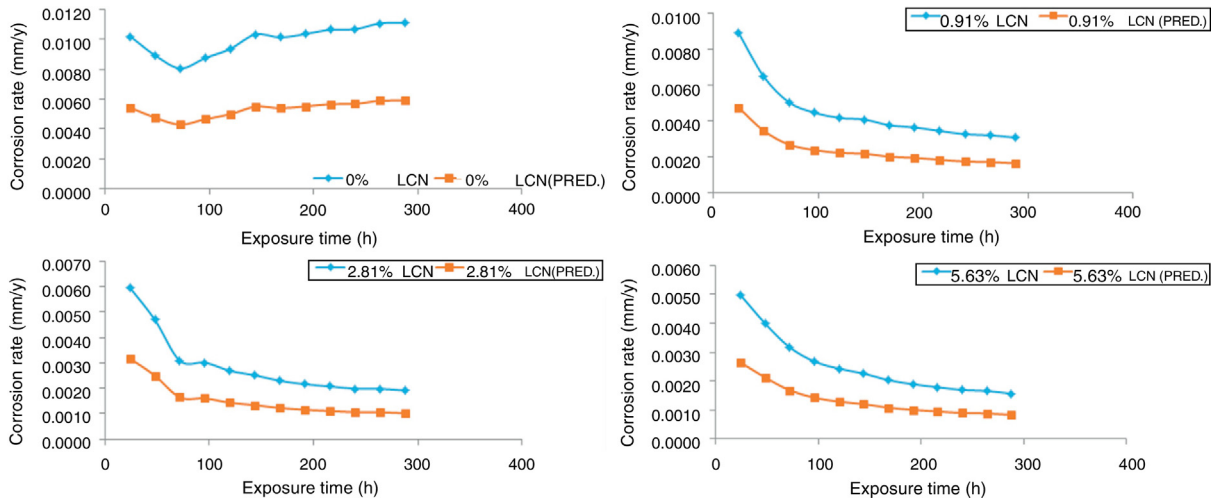

Fig. 9 – Plots of predicted and experimental corrosion rate results (a) 0% LCN, (b) 0.91% LCN, (c) 3.75% LCN and (d) 5.63% LCN.

correction factor expressing in terms of known experimental parameters as follows:

$$C_{Rm}\text{mod} = D_f\left(\frac{m/s \cdot kg/ms}{A * \rho}\right) = D_f\left(\frac{kg}{s * A * \rho}\right) \quad (17)$$

$$C_{Rm} = D_f\left(\frac{W_L}{T * A * \rho}\right) \quad (18)$$

D_f can be obtained by writing Eq. (18) in a straight line equation, $y = mx + c$ as

$$\ln\left(\frac{1}{C_R}\right) = \ln\left(\frac{A\rho}{D_f}\right) + \ln\left(\frac{T}{W_L}\right) \quad (19)$$

m is the slope of the equation and c is the intercept which corresponds to $\ln(A\rho/D_f)$. The experimental corrosion rate data of HCS in the acid solution at specific LCN concentrations in Table 6 was used to plot the graph of $\ln(1/C_R)$ vs $\ln(T/W_L)$. The Newton non-linear regression method of polymath was used to fit linear equation to the experimental plots was generated. The intercepts from those equations were equated to obtain the value of dimensionless corrosion rate correction factor (D_f) which was substituted in the developed empirical model equation for determining the theoretical corrosion rate values. The corrosion rate predicted by the model equations were plotted and compared with experimental corrosion rate in Figs.9–12. The predicted corrosion rates differed from the experimental corrosion rates by an average value of 53%.

4. Conclusion

LCN performed effectively on the corrosion inhibition of high carbon steel in HCl acid solution from potentiodynamic polarization analysis, weight loss test. Corrosion inhibition efficiency results were proportional to inhibitor concentration. The organic compound adsorbed onto the steel through chemisorption mechanism according to the Langmuir, Freundlich and Frumkin adsorption isotherm. Statistical analysis showed inhibitor concentration is the only relevant variable responsible for inhibition efficiency. Calculated results from predicted corrosion rate values varied from experimental results but followed the same trend. Identified functional groups completely adsorbed onto both steels from analysis of the adsorption spectra. The optical images of the inhibited steel samples slightly contrast the images without LCN compound.

Conflicts of interest

The author declares no conflicts of interest.

Acknowledgement

The author acknowledges Covenant University, Ota, Ogun State, Nigeria for the sponsorship and provision of research facilities for this project.

REFERENCES

[1] Mihit M, El Issami S, Bouklah M, Bazzi L, Hammouti B, Ait Addi E, et al. The inhibited effect of some tetrazolic compounds towards the corrosion of brass in nitric acid solution. Appl Surf Sci 2006;252(8):2389–95.
[2] Mihit M, Salghi R, El Issami S, Bazzi L, Hammouti B, Ait Addi E, et al. A study of tetrazoles derivatives as corrosion inhibitors of copper in nitric acid. Pigm Res Technol 2006;35(3):151–7.
[3] Dafali A, Hammouti B, Mokhlisse R, Kertit S. Influence of the cathodic intermetallics distribution on the reproducibility of the electrochemical measurements on AA5083 alloy in NaCl solutions. Corros Sci 2003;45(1):161–80.
[4] Kertit S, Salghi R, Bazzi L, Hammouti B, Bouchtart A. Electrochemical behaviour of aluminum alloy 3003 in carbonate solution in the presence of pyrazolic compounds. Ann Chim Sci Matér 2000;25(3):187–200.
[5] Gasparac R, Stupnisek-Lisac E. Corrosion protection on copper by imidazole and its derivatives. Corrosion 1999;55(11):1031–9.

Please cite this article in press as: Loto RT. Corrosion inhibition effect of non-toxic α-amino acid compound on high carbon steel in low molar concentration of hydrochloric acid. J Mater Res Technol. 2017. http://dx.doi.org/10.1016/j.jmrt.2017.09.005

[6] Moretti G, Guidi F, Grion G. Tryptamine as a green iron corrosion inhibitor in 0.5 M deaerated sulphuric acid. Corros Sci 2004;46(2):387–403.
[7] Zhang D, Gao L, Zhou G. Inhibition of copper corrosion in aerated hydrochloric acid solution by amino-acid compounds. J Appl Electrochem 2005;35(11):1081–5.
[8] Stupnisek-Lisac E, Loncaric Bozic A, Cafuk I. Low-toxicity copper corrosion inhibitors. Corrosion 1998;54(9): 713–20.
[9] Şahin M, Gece G, Karcı F, Bilgiç S. Experimental and theoretical study of the effect of some heterocyclic compounds on the corrosion of low carbon steel in 3.5% NaCl medium. J Appl Electrochem 2008;38(6):809–15.
[10] Rodríguez Valdez LM, Villamisar W, Casales M, González Rodriguez JG, Martínez Villafañe A, Martinez L, et al. Computational simulations of the molecular structure and corrosion properties of amidoethyl, aminoethyl and hydroxyethyl imidazolines inhibitors. Corros Sci 2006;48(12):4053–64.
[11] Agrawal YK, Talati JD, Shah MD, Desai MN, Shah NK. Schiff bases of ethylenediamine as corrosion inhibitors of zinc in sulphuric acid. Corros Sci 2004;46(3):633–51.
[12] Achary G, Sachin HP, Naik YA, Venkatesha TV. The corrosion inhibition of mild steel by 3-formyl-8-hydroxy quinoline in hydrochloric acid medium. Mater Chem Phys 2008;107(1):44–50.
[13] Varvara S, Rotaru I, Popa M, Muresan LM. Inhibition of bronze corrosion in aerated acidic solution using amino acids as environmentally friendly inhibitors. Rev Roum Chim 2011;56(7):793–801.
[14] Helal NH, Badawy WA. Environmentally safe corrosion inhibition of Mg–Al–Zn alloy in chloride free neutral solutions by amino acids. Electrochim Acta 2011;56(19):6581–7.
[15] Salghi R, Hammouti B, Kertit S, Bazzi L. Some amino acids as non-toxic inhibitors for the corrosion of aluminium alloy 6063 in dearated carbonate solution. Bull Electrochem 1997;13(10–11):399–404.
[16] Stupnisek-Lisac E, Brnada A, Mance AD. Secondary amines as copper corrosion inhibitors in acid media. Corros Sci 2000;42(2):243–57.
[17] Blajiev O, Hubin A. Inhibition of copper corrosion in chloride solutions by amino-mercapto-thiadiazol and methyl-mercapto-thiadiazol: an impedance spectroscopy and a quantum-chemical investigation. Electrochim Acta 2004;49(17–18):2761–70.
[18] Ramesh S, Rajeswari S. Evaluation of inhibitors and biocide on the corrosion control of copper in neutral aqueous environment. Corros Sci 2005;47(1):151–9.
[19] Scendo M. Potassium ethyl xanthate as corrosion inhibitor for copper in acidic chloride solutions. Corros Sci 2005;47(7):1738–49.
[20] Zerfaoui M, Oudda H, Hammouti B, Benkaddour M, Kertit S, Zertoubi M, et al. Electrochemical studies of the corrosion inhibition of methionine ethyl ester on iron in citric-chloride solution. La Rev Métall 2002;99(12):1105–10.
[21] Salghi R, Hammouti B, Aouinti A, Berrabah M, Kertit S. Aminoacid compounds as corrosion inhibitors for lead in 0.3 M HCl solution. J Electrochem Soc (India) 2000;49(1):40–2.
[22] Badawy WA, Ismail KM, Fathi AM. Corrosion control of Cu–Ni alloys in neutral chloride solutions by amino acids. Electrochim Acta 2006;51(20):4182–9.
[23] Ashassi-Sorkhabi H, Majidi MR, Seyyedi K. Investigation of inhibition effect of some amino acids against steel corrosion in HCl solution. Appl Surf Sci 2004;225(1–4):176–85.
[24] Zerfaoui M, Oudda H, Hammouti B, Kertit S, Benkaddour M. Inhibition of corrosion of iron in citric acid media by aminoacids. Progr Org Coat 2004;51(2):134–8.
[25] Abed Y, Hammouti B, Taled M, Kertit S. Corrosion inhibition of brass in nitric acid solution by Boc-phenyalanine. Trans SAEST 2002;37(3 & 4):92–102.
[26] ASTM G1-03. Standard practice for preparing, cleaning, and evaluating corrosion test specimens; 2011. http://www.astm.org/Standards/G1.
[27] ASTM G102-89. Standard practice for calculation of corrosion rates and related information from electrochemical measurements; 2015. http://www.astm.org/Standards/G31.
[28] Choi Y, Nesic S, Ling S. Effect of H_2S on the CO_2 corrosion of carbon steel in acidic solutions. Electrochim Acta 2011;56(4):1752–60.
[29] ASTM G31-12a. Standard practice for laboratory immersion corrosion testing of metals; 2012. https://www.astm.org/DATABASE.CART/HISTORICAL/G31-72R04.htm.
[30] Venkatesan P, Anand B, Matheswaran P. Influence of formazan derivatives on corrosion inhibition of mild steel in hydrochloric acid medium. E-J Chem 2009;6(S1):S438–44.
[31] Schutt HU, Horvath RJ. Crude column overhead corrosion problem caused by oxidized sulfur species. Houston, TX: NACE; 1987.
[32] Schofield MJ. Plant engineer's reference book. Elsevier; 2003.
[33] Cao C. On electrochemical techniques for interface inhibitor research. Corros Sci 1996;38(12):2073–82.
[34] Bockris JO, Drazic D, Despic AR. The electrode kinetics of the deposition and dissolution of iron. Electrochim Acta 1961;4(2–4):325–61.
[35] Bockris JO, Kita H. Analysis of galvanostatic transients and application to the iron electrode reaction. J Electrochem Soc 1961;108(7):676–85.
[36] El-Sayed A, Hossnia SM, Abd El-Lateef HM. The inhibition effect of 2,4,6-tris (2-pyridyl)-1,3,5-triazine on corrosion of tin, indium and tin–indium alloys in hydrochloric acid solution. Corros Sci 2010;52(6):1976–84.
[37] Refaey SAM, Taha F, Abd El-Malak AM. Corrosion and inhibition of 316 L stainless steel in neutral medium by 2-mercaptobenzimidazole. Int J Electrochem Sci 2006:80–91.
[38] Limousin G, Gaudet JP, Charlet L, Szenknect S, Barthes V, Krimissa M. Sorption isotherms: a review on physical bases, modeling and measurement. Appl Geochem 2007;22(2):249–75.
[39] Allen SJ, Mckay G, Porter JF. Adsorption isotherm models for basic dye adsorption by peat in single and binary component systems. J Colloid Interf Sci 2004;280(2):322–33.
[40] Refay SA, Taha F, Abd El-Malak AM. Inhibition of stainless steel pitting corrosion in acidic medium by 2-mercaptobenzoxazole. Appl Surf Sci 2004;236(1–4):175–85.
[41] Guidelli R. In: Kowski JL, Ross PN, editors. Adsorption of molecules at metal electrodes. New York: VCH Publishers Inc.; 1992. p. 1.
[42] Hosseini M, Stijn FLM, Mohammed RA. Synergism and antagonism in mild steel corrosion inhibition by sodium dodecylbenzenesulphonate and hexamethylenetetramine. Corros Sci 2003;45(7):1473–89.
[43] Ashish KS, Quraishi MA. Investigation of the effect of disulfiram on corrosion of mild steel in hydrochloric acid solution. Corros Sci 2011;53(4):1288–97.
[44] Zeldowitsch J. Adsorption site energy distribution. Acta Physicochim URSS 1934:961–73.
[45] Aharoni C, Ungarish M. Kinetics of activated chemisorption. Part 2. Theoretical models. J Chem Soc Faraday Trans 1 1977;73:456–64.
[46] Loto RT. Corrosion inhibition studies of the combined admixture of 1,3-diphenyl-2-thiourea and 4-hydroxy-3-methoxybenzaldehyde on mild steel in dilute acid media. Rev Colom Quim 2017;46(1):20–32.
[47] Loto RT, Loto CA, Popoola API, Fedotova T. Inhibition effect of butan-1-ol on the corrosion behavior of austenitic stainless

Please cite this article in press as: Loto RT. Corrosion inhibition effect of non-toxic α-amino acid compound on high carbon steel in low molar concentration of hydrochloric acid. J Mater Res Technol. 2017. http://dx.doi.org/10.1016/j.jmrt.2017.09.005

steel (Type 304) in dilute sulfuric acid. Arab J Chem 2015, http://dx.doi.org/10.1016/j.arabjc.2014.12.024.
[48] Oloche OB, Yaro SA, Okafor EG. Analytical correlation between varying corrosion parameters and corrosion rate of Al–4.5Cu/10%$ZrSiO_4$ composite in hydrochloric acid by rare earth chloride. J Alloys Compounds 2009;472(1–2):178–85.
[49] Johnson KE. Role of inclusions in the atmospheric pitting of stainless steel. Br Corros J 1981;15(3):123–7.
[50] Wan FYM. Mathematical models and their analysis. New York, USA: Harper and Row Publishers; 1989.
[51] Gibbings JC. Dimensional analysis. Springer; 2011.
[52] Akpa JG. Modeling of the corrosion rate of stainless steel in marine oil environment. ARPN J Eng Appl Sci 2013;8(8):656–62.
[53] Jayabharathy S, Pushparaj S, Mathiazhagan P. Prediction of corrosion rate of magnesium and its alloy-modeling. Int J Adv Res Basic Eng Sci Technol 2017;3(32):55–61.

Please cite this article in press as: Loto RT. Corrosion inhibition effect of non-toxic α-amino acid compound on high carbon steel in low molar concentration of hydrochloric acid. J Mater Res Technol. 2017. http://dx.doi.org/10.1016/j.jmrt.2017.09.005